

Formation of Metal–Cyanide Complexes in Deliquescent Airborne Particles: A New Possible Sink for HCN in Urban Environments

Chiara Giorio,^{*,†,‡,§} Daniele Marton,[†] Gianni Formenton,[§] and Andrea Tapparo[†]

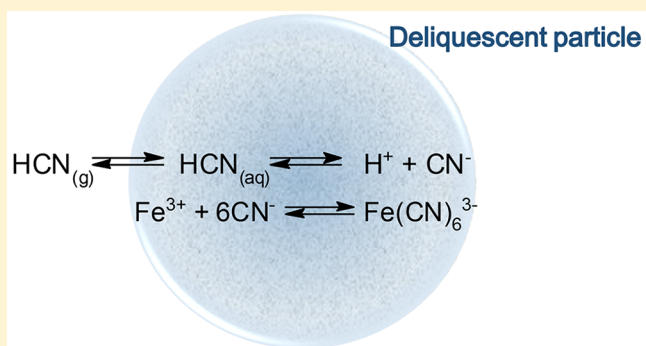
[†]Dipartimento di Scienze Chimiche, Università degli Studi di Padova, Via Marzolo 1, 35131 Padova, Italy

[‡]Aix Marseille Univ, CNRS, LCE, Marseille, 13331, France

[§]ARPAV Environmental Regional Agency, Laboratory Department, via Lissa 6, 30171 Mestre, Venice, Italy

Supporting Information

ABSTRACT: Hydrogen cyanide is a ubiquitous gas in the atmosphere and a biomass burning tracer. Reactive gases can be adsorbed onto aerosol particles where they can promote heterogeneous chemistry. In the present study, we report for the first time on the measurement and speciation of cyanides in atmospheric aerosol. Filter samples were collected at an urban background site in the city center of Padua (Italy), extracted and analyzed with headspace gas chromatography and nitrogen–phosphorus detection. The results showed that strongly bound cyanides were present in all aerosol samples at a concentration ranging between 0.3 and 6.5 ng/m³ in the PM_{2.5} fraction. The concentration of cyanides strongly correlates with concentration of total carbon and metals associated with combustion sources. The results obtained bring evidence that hydrogen cyanide can be adsorbed onto aerosol liquid water and can react with metal ions to form stable metal–cyanide complexes.



1. INTRODUCTION

Hydrogen cyanide (HCN) is a toxic gas which cause severe harm to human health.¹ It is approximately 20 times more toxic than carbon monoxide² and immediately dangerous to life or health at a concentration of 50 ppm and 25 mg/m³ as cyanide for most cyanide salts.³

HCN is a ubiquitous gas in the atmosphere^{4,5} with an average mixing ratio of ca. 200 ppt in nonpolluted environments.^{6,7} HCN is produced from pyrolysis of nitrogen containing organic matter. Its main source globally is biomass burning although the magnitude is still uncertain (0.1–3.2 Tg N/year)⁸ and it is considered a tracer of biomass burning together with CO and acetonitrile.^{9,10} Vehicular emissions, industrial processes and cigarette smoke are other minor tropospheric sources.^{7,8,11} Conversely, the large presence of HCN in Chinese urban plumes questions the suitability of HCN as biomass burning tracer in the lower troposphere where other sources, for example, residential coal burning, have been proposed to explain the observed high concentrations.⁷

In the atmosphere it is oxidized by OH radical and O(¹D) to form NO and N₂O thus contributing to the NO_x cycle.^{2,12} Other minor processes are photolysis and wet depositions.⁷ The major sink is uptake by ocean resulting in a tropospheric lifetime of about 5 months.^{6,7,10,13}

HCN is volatile (vapor pressure 742 mmHg at 25 °C)¹⁴ but it is known that reactive gases can be adsorbed onto particle surfaces where they can react with particle components.¹⁵ Water-soluble volatile organic compounds can also partition

into atmospheric aqueous phases, like cloud/fog droplets and deliquescent aerosol, where they can react with nonvolatile water-soluble aerosol components. For example, it has been shown that small carboxylic and dicarboxylic acids can coordinate with metal ions to form organic complexes.^{16,17}

A wide variety of organonitrogen compounds are found in the aerosol, which could be partially associated with heterogeneous reaction of HCN, although other mechanisms of formation are generally invoked, such as direct emissions from wood fires, and reaction of organics with NO_x and NH₃/NH₄⁺.¹⁸ Those compounds can produce CN[−] signals in online mass analyzers, e.g. in the aerosol time-of-flight mass spectrometer (ATOFMS).^{19–21} This signal has been associated with plant debris,²¹ oxidized nitrogen containing compounds²⁰ and organonitrogen from vehicular emissions¹⁹ as CN[−] signal in the ATOFMS is likely to be a fragment of higher molecular weight compounds.²¹ Up to now, measurement of cyanides in atmospheric aerosol has never been reported.

A method to measure total cyanides from stationary sources (particulate and gaseous emissions) has been published by the U.S. Environmental Protection Agency (EPA).²² This method has a detection limit of 0.01 mg/L in the extract²² and it is unsuitable for detection of cyanides in nonpolluted environ-

Received: June 19, 2017

Revised: November 13, 2017

Accepted: November 17, 2017

Published: November 17, 2017

ments where expected concentration of HCN in the gas phase is ca. 200 ppt.^{6,7} Recently, Marton et al.²³ published a new method for analysis of cyanides in industrial wastewaters which has a detection limit of 0.5 $\mu\text{g/L}$, 20 times lower than that of the EPA method,²² and allows speciation between available and total cyanides.²³ In aqueous systems, cyanides can be present as free cyanides (i.e., cyanide anions, hydrogen cyanide and its soluble salts), weak acid dissociable cyanides or WAD (i.e., weak cyanide complexes able to dissociate in a pH 4–6 range) and stable cyanide complexes (i.e., metal–cyanide complexes which are hydrolyzed under strong acid conditions, by heating or UV radiation).²³ The sum of free and WAD cyanides is also referred to as “available” cyanides.²³

In the present study, we adapted the method proposed by Marton et al.²³ to the analysis of available and total cyanides in aerosol samples collected in an urban background site in the city center of Padua (Italy). We report, for the first time, concentrations of cyanides in seasonal particulate matter (PM) samples, discussion of possible sources and multiphase reactions of hydrogen cyanide which allows it to enter into the particulate phase.

2. MATERIALS AND METHODS

2.1. Aerosol Sampling. Sampling campaigns were conducted at the university sampling site in Padua (Italy), in an urban background location in the Po Valley. More details about the sampling site can be found elsewhere.²⁴ 24 h concurrent samplings (from 9 am to 9 am of the following day) were carried out using a Zambelli Explorer Plus PM sampler fitted with a PM_{2.5} certified selector (CEN standard method UNI-EN14907) working at a constant flow rate of 2.3 m³/h and equipped with \varnothing 47 mm Teflon (PALL, Teflo Membrane, 1 μm pore size) or quartz fiber (AQFA, Millipore) filters. Sampling campaigns were conducted from the eighth November to 14th December 2006 (17 samples), from the 30th June to the 16th July 2009 (14 samples) and from the 12th January to the fourth February 2010 (17 samples). In addition PM₁₀ samples (CEN standard method UNI-EN12341) were collected from the eighth November to 14th December 2006 (17 samples), and PM₁ samples from the fifth November to 12th December 2007 (15 samples) according to the procedure already described elsewhere.²⁴

Filters were conditioned before and after sampling at a temperature of 20 ± 1 °C and relative humidity of $50 \pm 5\%$ (climatic box QBOX³ Momo Line) for at least 48 h. Samples were weighed daily using a microbalance (Ohaus Analytical Plus, sensitivity 10 μg) until constant mass was attained and then maintained at -20 °C until instrumental analysis (typical storage time <2 days).

Analysis of water-soluble ions, total metals and total carbon were done using the procedure already described elsewhere.²⁴

2.2. Analysis of Total and Available Cyanides. Determination of cyanides in aerosol samples was done by analyzing HCN released from the samples, after appropriate sample preparation, by static head space gas chromatography with nitrogen–phosphorus detection (HS-GC-NPD).

2.2.1. Sample Preparation. The extraction solution was prepared by adding 1 g of sulfamic acid ($\geq 99\%$, ReagentPlus, Sigma-Aldrich) and 25 mL of a pH 2 solution of phosphoric acid ($\geq 85\%$, ACS reagent, Sigma-Aldrich, Milan, Italy) to a 250 mL volumetric flask filled to the mark with water purified using a Millipore Milli-Q system (Vimodrone, Milan, Italy). 60 g of

sodium sulfate (anhydrous, $\geq 99.0\%$, Fluka, Milan, Italy) were then dissolved in the solution.

For sample preparation, $1/8$ of filter sample was placed in a 20 mL HS crimp-top glass vial and cooled down in liquid nitrogen for 30 s to minimize losses of HCN during sample preparation. Four milliliters of extraction solution were then added to the vial which was immediately crimped with an aluminum seal (\varnothing 20 mm, removable center, Supelco, Milan, Italy) fitted with a PTFE/silicone septum (\varnothing 20 mm, Supelco), and vigorously shaken. For analysis of available cyanides, samples were placed in a thermostatic bath (F3-Q Haake-Thermostate, Fisons, Ipswich, UK) at 25 ± 0.1 °C while for analysis of total-cyanides the samples were treated at 140 ± 1 °C in a Memmert UFB 400 oven (Schwabach, Germany) for 1 h and then quickly cooled in a thermostatic bath at 25 ± 0.1 °C as optimized in a previous study.²³ In both cases, instrumental analysis was performed after an equilibration time of at least 24 h at 25 ± 0.1 °C. Details about optimization and validation of the sample preparation method, sampling artifacts and recovery tests are reported in the Supporting Information (SI).

2.2.2. Instrumental Analysis. Instrumental analysis was performed using the method already described elsewhere.²³ Briefly, 0.8 mL of static HS phase, collected with a 1 mL Hamilton gastight syringe (1001 RN, Hamilton, Bonaduz, Switzerland), was injected directly in a quartz deactivated liner (L 86 mm, o.d. 4 mm, i.d. 2 mm, PerkinElmer) maintained at 100 °C and 14 psi with N₂ carrier gas at 1.31 mL/min, with split ratio 1:5, in a Autosystem XL (PerkinElmer, Monza, Italy) gas chromatograph equipped with a Nitrogen–Phosphorus Detector (NPD).

A DVB Supel-Q PLOT (Supelco) capillary column (30 m \times 0.32 mm \times 0.25 μm) was used for separation. Oven temperature was held at 50 °C for 6 s after sample injection and then ramped at 45 °C/min to 230 °C and held for 1 min. Detector temperature and voltage were 250 °C and ~ 1 mV, with 100 mL/min and 1.7 mL/min of air flow and H₂ flow, respectively. The chromatographic run lasted about 5.5 min. After each run, the syringe was washed under N₂ flow to avoid memory effects.²³

External calibration (five calibration levels) was performed daily by analyzing 0.8 mL of equilibrated HS phase of standard solutions prepared using the same procedure described for real samples, in the calibration range 0–10 $\mu\text{g/L}$ by diluting a certified standard solution of NaCN or K₃[Fe(CN)₆] at 1000 ± 2 mg/L concentration (as cyanide) purchased from Ultra-Scientific Analytical Solutions (Bologna, Italy).

2.2.3. Safety Precautions. The acute toxicity of HCN requires adoption of safety measures to avoid release of gaseous HCN in the working environment, despite the very low concentrations of both samples and standard solutions. Preparation of both standards and samples needs to be carried out under a fume cupboard. Cyanide standards should be stored away from acidic solutions to avoid accidental mixing. After use, all solutions should be disposed in a dedicated waste container with hypochlorite and excess NaOH to avoid release of HCN.²³

2.3. Calculation of Aerosol Liquid Water Content. Average aerosol liquid water (ALW) content, in mass concentration, was calculated using the comprehensive version of the model E-AIM IV available online (<http://www.aim.env.uea.ac.uk/aim/aim.php>).^{25–27} The E-AIM model has recently been shown to agree well with independent measured data.²⁸ 24h averaged data for temperature, relative humidity (obtained

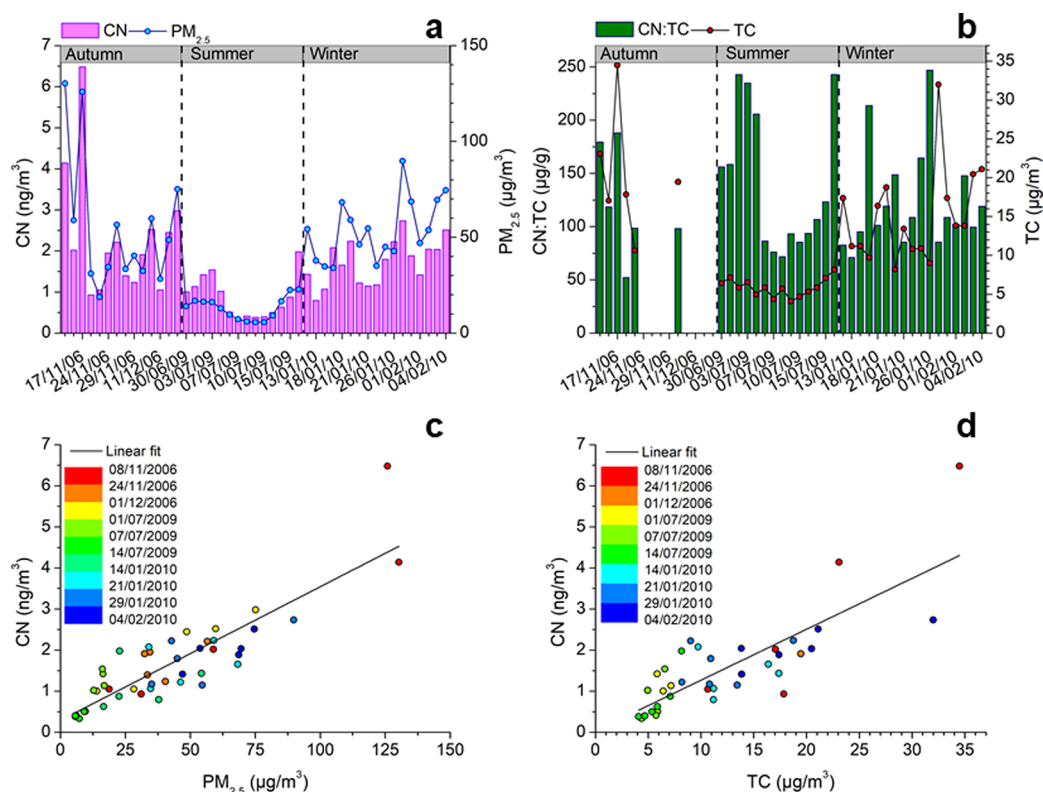


Figure 1. Timeseries of the daily concentrations of cyanides compared with concentrations of PM_{2.5} (a) and timeseries of CN/TC compared with concentrations of TC (b) in autumn 2006, summer 2009 and winter 2010; correlation between CN concentrations and PM_{2.5} concentrations (c) and correlation between CN concentrations and TC concentrations (d) in autumn 2006, summer 2009 and winter 2010.

from ARPA Veneto, the Regional Environmental Agency), amounts of ammonium, sodium, chloride, nitrate, and sulfate were considered for calculation of water uptake. Proton and ammonia amounts were calculated to obtain charge neutrality. Oxalic acid was also considered for calculation of water uptake in both its undissociated and dissociated forms. Dissociation of oxalic acid was calculated based on the pH and equilibria between the main ions measured in the aerosol samples.

2.4. Principal Component Analysis. Principal component analysis (PCA) was done using Statistica 10 (StatSoft Inc., Tulsa, OK) on all PM_{2.5} samples and species analyzed. Temperature, relative humidity and ALW were used as supplementary variables. The first two principal components (PC) were selected on the basis of the scree plot (not shown), explaining the 76.4% of the variance of the data set (62.2% by PC 1 and 14.2% by PC 2).

3. RESULTS AND DISCUSSION

3.1. Speciation, Concentrations and Seasonality of Cyanides in Urban PM_{2.5}. The results of the analysis showed the presence of strongly bound cyanides in all PM_{2.5} samples. Concentrations of cyanides in PM_{2.5} ranged from 0.3 to 6.5 ng/m³, with a median value of 1.4 ng/m³, and 25th and 75th percentiles of 1.0 and 2.1 ng/m³ respectively. Conversely, available cyanides were not detected in any analyzed aerosol sample. This can be explained in two ways. First, adsorbed HCN and WAD cyanides may be lost during postsampling conditioning of the filters (see SI section S1.1.4). Second, HCN is very volatile, and WAD cyanides can be dissociated at the pH expected for aerosol samples,²⁹ releasing HCN, which would be revolatilised into the gas phase even during sampling

operations. Therefore, the cyanides detected in this series of samples are in stable metal–ligand complexes that cannot be dissociated at weak acidic conditions. For example, stable metal–cyanide complexes are those with transition metal ions (in particular iron) commonly present in aerosol from different locations/sources.

The potential loss of semivolatile and volatile CN species during sampling operations reflects mechanisms and processes that normally occur on aerosol particles, and affect their chemical composition. We can hypothesize that, during sampling, gas-particle partitioning can modify HCN concentrations (adsorption of HCN onto particle surfaces and loss of HCN back to the gas phase) in the same manner in which gas-particle partitioning occurs and modify HCN concentrations under normal atmospheric conditions. Henry's law suggests that HCN is very soluble in water despite its volatility ($K_H = 9.94 \text{ M/atm}$ at 25 °C, corresponding to a dimensionless value of $K_H = C_{\text{air}}/C_{\text{water}} = 4 \times 10^{-3}$)²³ so, if present in the particles HCN and weak cyanide complexes should be detected, as free or WAD cyanides, and not completely lost during sampling. The fact that we never detect available CN in our samples is due to the scarce significance of this fraction in the atmospheric particles themselves. This is not surprising as the formation of weak-acid dissociable complexes would not be favored on acidic deliquescent particles.

The timeseries of total cyanide concentrations in PM_{2.5} are reported in Figure 1. Concentration of strongly bound cyanides in PM_{2.5} showed a seasonal trend characterized by lower concentrations in the summer. Concentrations were on average $2.3 \pm 1.5 \text{ ng/m}^3$ in autumn 2006, $0.9 \pm 0.5 \text{ ng/m}^3$ in summer 2009, and $1.7 \pm 0.6 \text{ ng/m}^3$ in winter 2010. Cyanides are

moderately anticorrelated with temperature ($r = -0.37, p < 0.05$) as lower temperatures favor partitioning of volatile species onto the particle surface explaining lower concentrations during the summer. Concentrations of total cyanides are strongly correlated with $PM_{2.5}$ concentrations ($r = 0.86, p < 0.001$) and with concentrations of total carbon ($r = 0.81, p < 0.001$). The CN^-/TC ratio remained constant throughout the campaigns with an average of $0.13 \pm 0.05 \mu\text{g/g}$ and no significant differences between different seasons.

3.2. Size Segregation, Correlation with Other Variables and Possible Sources. In the autumn 2006 campaign, concurrent PM_{10} and $PM_{2.5}$ samples were collected and analyzed for the presence of total cyanides. The results of the analysis showed no differences in concentrations of strongly bound cyanides in $PM_{2.5}$ and PM_{10} (t -paired test, $p = 0.96$), indicating that cyanides are present in the fine fraction. However, the coarse fraction of PM itself was scarcely represented in our samples where $PM_{2.5}/PM_{10}$ was ~ 0.9 on average, and in the coarse fraction metals are probably less soluble due to the relative high stability of the crustal component, therefore they are not prone to react with cyanides.

The presence of cyanides in the fine fraction of PM is consistent with a strong correlation with TC concentrations ($r = 0.81, p < 0.001$). Cyanides are correlated also with species related to combustion sources as pointed out by the results of the PCA (Figure 2). Results of the PCA analysis run on $PM_{2.5}$ samples from all three seasons show the presence of three main

groups of variables in the plane defined by the first two PC (Figure 2a). These three groups can be linked to crustal material (yellow circle), combustion sources (red circle) and secondary processes (blue circle). Cyanides point toward the same direction as $PM_{2.5}$, TC and ions that can be related to combustion sources including biomass burning (e.g., K^+ , NH_4^+). As expected, sodium and chloride point also in the direction of combustion sources and do not seem to be associated with sea spray. PCA results show also that summer samples (red square in Figure 2b) are divided from the winter and autumn samples (blue square) along the axis defined by PC 1.

Samples of PM_{10} and $PM_{2.5}$ for the autumn 2006 campaign and PM_1 samples from autumn 2007 were analyzed also with ICP-MS. Cyanides present moderate to strong correlations with many metals with the exception of Mo and Sb (Table 1).

Table 1. Correlations (r)^a between Concentrations of Cyanides and Concentrations of Metals in PM_{10} and $PM_{2.5}$ Samples Collected in Autumn 2006 and PM_1 Samples Collected in Autumn 2007

metals	r (CN vs metals)			possible sources of metals
	PM_{10}	$PM_{2.5}$	PM_1	
Mn	0.88	0.43	0.61	road dust, vehicle emissions, tire wear ³² , coal/oil combustion ³³ , smelting ³³ , steel/Cd industry ³³
Ni	0.75	0.70	0.39	road dust ³² , vehicle emissions ³² , coal-oil combustion ³³ , smelting ³³
Cu	0.51	0.47	0.68	vehicle emissions ³² , smelting ³³ , brake wear ³⁴
Zn	0.58	0.66	0.74	tire wear ³² , coal-oil combustion ³³ , biomass burning ³⁰
As	0.74	0.83	0.09	industry ³² , biomass burning ³⁰
Se	0.58	0.34	0.70	fossil fuels, coal fired power plants, coal fly ash, biomass burning ³¹ , tire wear ³²
Br	0.55	0.41	0.19	road dust ³²
Rb	0.64	0.56	0.87	biomass burning ³⁰
Mo	0.17	0.00	0.27	oil combustion ³⁰
Cd	0.18	0.91	0.03	coal-oil combustion ³³ , steel/Cd industry ³³ , biomass burning ³⁰
Sb	0.32	0.45	-0.15	brake wear ³⁴
Ba	0.32	0.17	0.82	vehicle emissions ³² , brake wear ³⁴⁻³⁶
Pb	0.76	0.76	0.48	industry ³² , coal/oil combustion ³³
V	0.62	0.54	0.19	road dust ³² , fuel/oil combustion ³⁷
Cr	0.56	0.69	0.86	soil/road dust ³³ , brake and tire wear, steel production ³⁸
Fe	0.58	0.41	0.71	vehicle emissions, road dust, tire wear ³² , soil/road dust ³³ , brake wear ³⁴

^aStrong correlations ($r > 0.5$) are highlighted in bold.

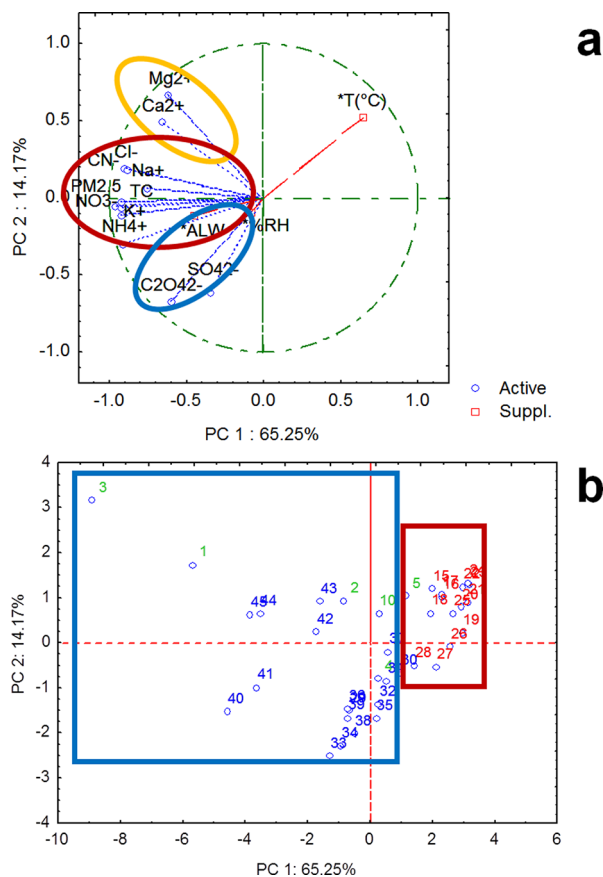


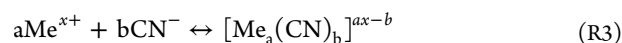
Figure 2. Results of PCA analysis as loadings (a) and scores (b) referred to the first two principal components. Red square indicates summer samples and blue square indicates autumn and winter samples.

Cyanides were present in the fine fraction of PM, therefore differences in the correlation strength with metals in PM_{10} and $PM_{2.5}$ are linked to differences in metal content in the two fractions and not to cyanide content. As expected, cyanides are strongly correlated with all metals that can be associated with biomass burning emissions, like Zn, As, Se, Rb, and Cd.^{30,31} In addition, cyanides correlate with metals that can be associated with vehicular emissions, like Mn, Ni, Cu, Se, Ba, V, and Fe.^{31,32} Our results suggest that cyanides are not linked only to biomass burning but also other combustion sources, like vehicular emissions and house heating, can contribute to the observed concentrations. This is in agreement with the large presence of HCN in Chinese urban plumes, which were tentatively linked to residential coal burning.⁷ Correlations between cyanides and

metals can also be due to formation of metal–cyanide complexes in atmospheric particles (see section 3.3).

3.3. Mechanism of Partitioning into the Condensed Phase and Atmospheric Implications. In all analyzed samples, cyanides were present in the form of stable metal–ligand complexes (see section 3.1), however, to the authors' knowledge, no primary emission sources of stable cyanide complexes exist. In addition, the strong anticorrelation of cyanide concentrations with temperatures (section 3.1) and strong correlations with TC and metals associated with combustion sources (sections 3.1 and 3.2) suggest that cyanides enter into the condensed phase via multiphase chemistry, after adsorption of HCN onto particles. Therefore, cyanide concentration in the particles is dependent upon metal concentrations, especially for those metals that can form stable cyanide complexes, and its correlation with metals may result from this atmospheric mechanism. Lower temperatures favor the repartitioning of volatile species onto particle surfaces, but also dissolution of HCN in water as the Henry's law constant increases with lower temperatures.³⁹

On these basis, we hypothesize that cyanides complexes form in the particles after partitioning of HCN from the gas phase onto deliquescent aerosol particles, its dissolution in water^{39,40} and subsequent dissociation to form cyanide anions, which then can react with transition metal ions to form metal–cyanide complexes. The overall process is represented by the reactions R1–R3, where Me^{x+} represents a generic metal ion with unknown charge.



It is believed that the acidic conditions of ALW would favor protonation of CN^- and limit the formation of metal–cyanide complexes in the aerosol phase.⁴¹ However, HCN is water-soluble^{23,39,40} and formation of stable metal–ligand complexes can shift this equilibrium and increase the dissolution of HCN.

In order to test the hypothesized mechanism, the ALW content of all $\text{PM}_{2.5}$ samples was calculated using E-AIM (details in section 2.3). In general, our values of ALW content (see SI Table S2) are comparable with the maximum concentrations obtained in urban sites in previous studies, like for example those of Beijing and Manchester.⁴² During the autumn and winter campaigns, a few days were characterized by very high ALW concentrations, around $100 \mu\text{g}/\text{m}^3$ and above, and $T - T_d < 2 \text{ }^\circ\text{C}$ (where T_d is the dew temperature calculated using the method from Lawrence⁴³) suggesting high likelihood to have fog formation.

Concentrations of cyanides in $\text{PM}_{2.5}$ are not strongly correlated ($r = 0.45$, $p = 0.002$) with the ALW content, according to the classification proposed by Cohen.⁴⁴ Days in which there was a high likelihood of fog formation were characterized by relatively high, but not necessarily, peak concentrations of cyanides suggesting that other factors besides the amount of ALW play a role in the metal–cyanide complexes formation. Such factors could be concentrations of metal ions, pH, temperature, and amount of oxidants which could react with and therefore consume HCN.

Among these factors, the concentrations of metals that can form stable metal–cyanide complexes are likely to play a key role. For those $\text{PM}_{2.5}$ samples for which the concentration of

metals is available ($\text{PM}_{2.5}$ samples collected during the autumn 2006 campaign), the correlation between the concentrations of cyanides and ALW is not strong ($r = 0.53$, $p = 0.049$) and the correlation between the concentrations of cyanides and Fe, the most abundant metal able to form strong complexes with cyanides, is not strong also ($r = 0.40$, $p = 0.148$). However, if we consider the sum of Fe and ALW (both normalized), the correlation with the concentrations of cyanides becomes strong ($r = 0.71$, $p = 0.004$). This result supports our hypothesis that cyanides enter into the particle phase through an aqueous phase process in deliquescent particles. The dependence of the concentrations of cyanides on the concentrations of both ALW and Fe is shown in Figure 3 and the timeseries are shown in SI

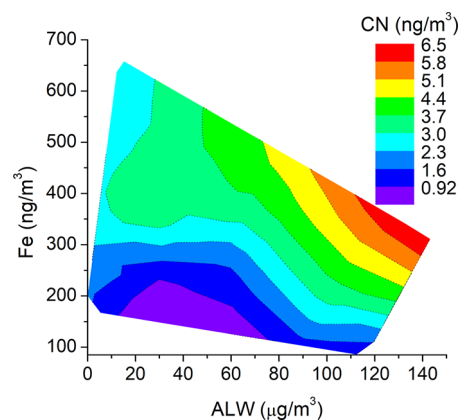


Figure 3. Contour plot showing the dependence of CN concentrations on both ALW and Fe concentrations in $\text{PM}_{2.5}$ collected in autumn 2006.

Figure S3. It can be seen from Figure 3 that in days characterized by high ALW content but low Fe concentrations, concentrations of cyanides are also low. Likewise, in days characterized by low ALW content but high Fe concentrations, concentrations of cyanides are also low. Peak concentrations of cyanides occur when enough iron is solubilized into the aerosol water to promote formation of iron–cyanide complexes.

Our study brings evidence of the formation of metal–cyanide complexes in deliquescent aerosol particles in an urban environment. This mechanism suggests a new sink for HCN in urban environments. HCN is considered a tracer from biomass burning,^{9,10} however current global atmospheric models suggest the presence of a missing source or an underestimation of the sources of HCN.⁴⁵ The correlations between metals and cyanides in the particles are likely due to the mechanism by which the cyanides enter into the particle phase rather than a common emission source, therefore our results do not give indication of new possible sources. On a global scale, the main sink of HCN in the lower troposphere is through uptake by oceans, presumably through biological degradation, with minor contributions from photochemistry and wet depositions,^{7,45} while in the upper troposphere and in the stratosphere main sinks are through reactions with $\cdot\text{OH}$ and $\text{O}(^1\text{D}_2)$.¹² More studies are now needed to investigate the importance of the mechanism proposed here as a sink of HCN in the lower troposphere and the parameters influencing the formation of metal–cyanide complexes in deliquescent aerosol and eventually cloud droplets.

In the case of cyanides, formation of strong metal–ligand complexes represents a detoxification mechanism as the toxicity

of metal–cyanide complexes is associated with their ability to release free CN^- and HCN .⁴⁶ The possible formation of metal–organic complexes in PM was postulated in previous studies,^{16,17,41} however this represents the first time in which experimental evidence of the occurrence of such mechanism in atmospheric aerosol is brought. Many water-soluble organic and inorganic compounds already present in the aerosol have coordinating properties toward metal ions, and they can increase their solubility.⁴¹ Notable examples of aerosol components having coordinating properties are highly oxidized organic compounds, such as low molecular weight hydroxy-, oxo-, and dicarboxylic acids as well as dicarbonyls,^{41,47,48} and macromolecules like humic-like and fulvic-like substances⁴⁹ and oligomers.^{50–53} The evidence that some metal–ligand complexes are formed in the aerosol from independent precursors, open new interesting perspectives for the study of the toxic properties of metal containing particles.

■ ASSOCIATED CONTENT

● Supporting Information

The Supporting Information is available free of charge on the ACS Publications website at DOI: 10.1021/acs.est.7b03123.

Additional experimental details and results, including two figures and six tables (PDF)

■ AUTHOR INFORMATION

Corresponding Author

*E-mail: chiara.giorio@unipd.it.

ORCID

Chiara Giorio: 0000-0001-7821-7398

Notes

The authors declare no competing financial interest.

■ ACKNOWLEDGMENTS

Authors are grateful to Alessandro Dalla Libera, and Fabio Santacatterina for initial tests and measurements.

■ REFERENCES

- (1) United States Environmental Protection Agency. Cyanide Compounds - Hazard Summary <https://www.epa.gov/sites/production/files/2016-09/documents/cyanide-compounds.pdf> (accessed October 23, 2017).
- (2) Dagaut, P.; Glarborg, P.; Alzueta, M. The oxidation of hydrogen cyanide and related chemistry. *Prog. Energy Combust. Sci.* **2008**, *34* (1), 1–46.
- (3) ATSDR. Public Health Statement for Cyanide <https://www.atsdr.cdc.gov/ToxProfiles/tp8-c1-b.pdf>.
- (4) Coffey, M. T.; Mankin, W. G.; Cicerone, R. J. Spectroscopic detection of stratospheric hydrogen cyanide. *Science* **1981**, *214* (4518), 333–335.
- (5) Cicerone, R. J.; Zellner, R. The atmospheric chemistry of hydrogen cyanide (HCN). *J. Geophys. Res.* **1983**, *88* (C15), 10689.
- (6) Baum, M. M.; Moss, J. A.; Pastel, S. H.; Poskrebyshev, G. A. Hydrogen Cyanide Exhaust Emissions from In-Use Motor Vehicles. *Environ. Sci. Technol.* **2007**, *41* (3), 857–862.
- (7) Li, Q. A global three-dimensional model analysis of the atmospheric budgets of HCN and CH₃CN: Constraints from aircraft and ground measurements. *J. Geophys. Res.* **2003**, *108* (D21), 8827.
- (8) Li, Q.; Palmer, P. I.; Pumphrey, H. C.; Bernath, P.; Mahieu, E. What drives the observed variability of HCN in the troposphere and lower stratosphere? *Atmos. Chem. Phys.* **2009**, *9* (21), 8531–8543.
- (9) Le Breton, M.; Bacak, A.; Muller, J. B. A.; O'Shea, S. J.; Xiao, P.; Ashfold, M. N. R.; Cooke, M. C.; Batt, R.; Shallcross, D. E.; Oram, D. E.; et al. Airborne hydrogen cyanide measurements using a chemical ionisation mass spectrometer for the plume identification of biomass burning forest fires. *Atmos. Chem. Phys.* **2013**, *13* (18), 9217–9232.
- (10) Shim, C.; Wang, Y.; Singh, H. B.; Blake, D. R.; Guenther, A. B. Source characteristics of oxygenated volatile organic compounds and hydrogen cyanide. *J. Geophys. Res.* **2007**, *112* (D10), D10305.
- (11) Bigourd, D.; Cuisset, A.; Hindle, F.; Matton, S.; Fertein, E.; Bocquet, R.; Mouret, G. Detection and quantification of multiple molecular species in mainstream cigarette smoke by continuous-wave terahertz spectroscopy. *Opt. Lett.* **2006**, *31* (15), 2356.
- (12) Strekowski, R. S.; Nicovich, J. M.; Wine, P. H. Kinetic and Mechanistic study of the Reactions of O(1D₂) with HCN and CH₃CN. *ChemPhysChem* **2010**, *11* (18), 3942–3955.
- (13) Singh, H. B. In situ measurements of HCN and CH₃CN over the Pacific Ocean: Sources, sinks, and budgets. *J. Geophys. Res.* **2003**, *108* (D20), 8795.
- (14) Daubert, T. E.; Danner, R. P. *Physical and Thermodynamic Properties of Pure Chemicals: Data Compilation*; Taylor & Francis: Washington, DC, 1989.
- (15) Kolb, C. E.; Cox, R. A.; Abbatt, J. P. D.; Ammann, M.; Davis, E. J.; Donaldson, D. J.; Garrett, B. C.; George, C.; Griffiths, P. T.; Hanson, D. R.; et al. An overview of current issues in the uptake of atmospheric trace gases by aerosols and clouds. *Atmos. Chem. Phys.* **2010**, *10* (21), 10561–10605.
- (16) Deguillaume, L.; Leriche, M.; Desboeufs, K.; Mailhot, G.; George, C.; Chaumerliac, N. Transition metals in atmospheric liquid phases: Sources, reactivity, and sensitive parameters. *Chem. Rev.* **2005**, *105*, 3388–3431.
- (17) Scheinhardt, S.; Müller, K.; Spindler, G.; Herrmann, H. Complexation of trace metals in size-segregated aerosol particles at nine sites in Germany. *Atmos. Environ.* **2013**, *74*, 102–109.
- (18) Ito, A.; Lin, G.; Penner, J. E. Global modeling study of soluble organic nitrogen from open biomass burning. *Atmos. Environ.* **2015**, *121*, 103–112.
- (19) Giorio, C.; Tapparo, A.; Dall'Osto, M.; Beddows, D. C. S.; Esser-Gietl, J.; Healy, R. M.; Harrison, R. M. Local and regional components of aerosol in a heavily trafficked street canyon in central London derived from PMF and cluster analysis of single particle ATOFMS spectra. *Environ. Sci. Technol.* **2015**, *39*, 3330–3340.
- (20) Giorio, C.; Tapparo, A.; Dall'Osto, M.; Harrison, R. M.; Beddows, D. C. S.; Di Marco, C.; Nemitz, E. Comparison of three techniques for analysis of data from an Aerosol Time-of-Flight Mass Spectrometer. *Atmos. Environ.* **2012**, *61*, 316–326.
- (21) Dall'Osto, M.; Harrison, R. M. Chemical characterisation of single airborne particles in Athens (Greece) by ATOFMS. *Atmos. Environ.* **2006**, *40* (39), 7614–7631.
- (22) EPA. Method 426 Determination of Cyanide Emissions from Stationary Sources <http://www.arb.ca.gov/testmeth/vol3/meth426.pdf>.
- (23) Marton, D.; Tapparo, A.; Di Marco, V. B.; Repice, C.; Giorio, C.; Bogianni, S. Ultratrace determination of total and available cyanides in industrial wastewaters through a rapid headspace-based sample preparation and gas chromatography with nitrogen phosphorous detection analysis. *J. Chromatogr. A* **2013**, *1300* (0), 209–216 <http://dx.doi.org/10.1016/j.chroma.2013.03.004>.
- (24) Giorio, C.; Tapparo, A.; Scapellato, M. L.; Carrieri, M.; Apostoli, P.; Bartolucci, G. B. Field comparison of a personal cascade impactor sampler, an optical particle counter and CEN-EU standard methods for PM₁₀, PM_{2.5} and PM₁ measurement in urban environment. *J. Aerosol Sci.* **2013**, *65*, 111–120.
- (25) Friese, E.; Ebel, A. Temperature Dependent Thermodynamic Model of the System $\text{H}^+ - \text{NH}_4^+ - \text{Na}^+ - \text{SO}_4^{2-} - \text{NO}_3^- - \text{Cl}^- - \text{H}_2\text{O}$. *J. Phys. Chem. A* **2010**, *114* (43), 11595–11631.
- (26) Wexler, A. S. Atmospheric aerosol models for systems including the ions H^+ , NH_4^+ , Na^+ , SO_4^{2-} , NO_3^- , Cl^- , Br^- , and H_2O . *J. Geophys. Res.* **2002**, *107* (D14), 4207.
- (27) Clegg, S. L.; Pitzer, K. S.; Brimblecombe, P. Thermodynamics of multicomponent, miscible, ionic solutions. Mixtures including unsymmetrical electrolytes. *J. Phys. Chem.* **1992**, *96* (23), 9470–9479.

- (28) Engelhart, G. J.; Hildebrandt, L.; Kostenidou, E.; Mihalopoulos, N.; Donahue, N. M.; Pandis, S. N. Water content of aged aerosol. *Atmos. Chem. Phys.* **2011**, *11* (3), 911–920.
- (29) Keene, W. C.; Pszenny, A. A. P.; Maben, J. R.; Stevenson, E.; Wall, A. Closure evaluation of size-resolved aerosol pH in the New England coastal atmosphere during summer. *J. Geophys. Res.* **2004**, *109* (D23), D23307.
- (30) Landis, M. S.; Patrick Pancras, J.; Graney, J. R.; White, E. M.; Edgerton, E. S.; Legge, A.; Percy, K. E. Source apportionment of ambient fine and coarse particulate matter at the Fort McKay community site, in the Athabasca Oil Sands Region, Alberta. *Sci. Total Environ.* **2017**, *584–585*, 105–117.
- (31) De Santiago, A.; Longo, A. F.; Ingall, E. D.; Diaz, J. M.; King, L. E.; Lai, B.; Weber, R. J.; Russell, A. G.; Oakes, M. Characterization of Selenium in Ambient Aerosols and Primary Emission Sources. *Environ. Sci. Technol.* **2014**, *48* (16), 8988–8994.
- (32) Jeong, C.-H.; Wang, J. M.; Evans, G. J. Source Apportionment of Urban Particulate Matter using Hourly Resolved Trace Metals, Organics, and Inorganic Aerosol Components. *Atmos. Chem. Phys. Discuss.* **2016**, No. April, 1–32.
- (33) Lee, B.-K. Seasonal Variation and Sources of Heavy Metals in Atmospheric Aerosols in a Residential Area of Ulsan, Korea. *Aerosol Air Qual. Res.* **2011**, *11* (6), 679–688.
- (34) Hagino, H.; Oyama, M.; Sasaki, S. Laboratory testing of airborne brake wear particle emissions using a dynamometer system under urban city driving cycles. *Atmos. Environ.* **2016**, *131*, 269–278.
- (35) Monaci, F.; Bargagli, R. Barium and other trace metals as indicators of vehicle emissions. *Water, Air, Soil Pollut.* **1997**, *100* (1–2), 89–98.
- (36) Gietl, J. K.; Lawrence, R.; Thorpe, A. J.; Harrison, R. M. Identification of brake wear particles and derivation of a quantitative tracer for brake dust at a major road. *Atmos. Environ.* **2010**, *44* (2), 141–146.
- (37) Shafer, M. M.; Toner, B. M.; Overdier, J. T.; Schauer, J. J.; Fakra, S. C.; Hu, S.; Herner, J. D.; Ayala, A. Chemical speciation of vanadium in particulate matter emitted from diesel vehicles and urban atmospheric aerosols. *Environ. Sci. Technol.* **2012**, *46* (1), 189–195.
- (38) Byrne, P.; Taylor, K. G.; Hudson-Edwards, K. A.; Barrett, J. E. S. Speciation and potential long-term behaviour of chromium in urban sediment particulates. *J. Soils Sediments* **2017**, *17* (11), 2666–2676.
- (39) Ma, J.; Dasgupta, P. K.; Blackledge, W.; Boss, G. R. Temperature dependence of Henry's law constant for hydrogen cyanide. Generation of trace standard gaseous hydrogen cyanide. *Environ. Sci. Technol.* **2010**, *44* (8), 3028–3034.
- (40) Sander, R. Compilation of Henry's law constants (version 4.0) for water as solvent. *Atmos. Chem. Phys.* **2015**, *15* (8), 4399–4981.
- (41) Okochi, H.; Brimblecombe, P. Potential trace metal-organic complexation in the atmosphere. *Sci. World J.* **2002**, *2*, 767–786.
- (42) Nguyen, T. K. V.; Zhang, Q.; Jimenez, J. L.; Pike, M.; Carlton, A. G. Liquid water: Ubiquitous contributor to aerosol mass. *Environ. Sci. Technol. Lett.* **2016**, *3* (7), 257–263.
- (43) Lawrence, M. G. The relationship between relative humidity and the dewpoint temperature in moist air: A simple conversion and applications. *Bull. Am. Meteorol. Soc.* **2005**, *86* (2), 225–233.
- (44) Cohen, J. *Statistical Power Analysis for the Behavioral Sciences*; Lawrence Erlbaum Associates Inc.: New Jersey, 1988.
- (45) Lupu, A.; Kaminski, J. W.; Neary, L.; McConnell, J. C.; Toyota, K.; Rinsland, C. P.; Bernath, P. F.; Walker, K. A.; Boone, C. D.; Nagahama, Y.; et al. Hydrogen cyanide in the upper troposphere: GEM-AQ simulation and comparison with ACE-FTS observations. *Atmos. Chem. Phys.* **2009**, *9* (13), 4301–4313.
- (46) Jaszczak, E.; Polkowska, Ż.; Narkowicz, S.; Namieśnik, J. Cyanides in the environment—analysis—problems and challenges. *Environ. Sci. Pollut. Res.* **2017**, *24* (19), 15929–15948.
- (47) Brégonzio-Rozier, L.; Siekmann, F.; Giorio, C.; Pangu, E.; Morales, S. B.; Temime-Roussel, B.; Gratien, A.; Michoud, V.; Ravier, S.; Cazaunau, M.; et al. Gaseous products and secondary organic aerosol formation during long term oxidation of isoprene and methacrolein. *Atmos. Chem. Phys.* **2015**, *15*, 2953–2968.
- (48) Brégonzio-Rozier, L.; Giorio, C.; Siekmann, F.; Pangu, E.; Morales, S. B.; Temime-Roussel, B.; Gratien, A.; Michoud, V.; Cazaunau, M.; DeWitt, H. L.; et al. Secondary organic aerosol formation from isoprene photooxidation during cloud condensation–evaporation cycles. *Atmos. Chem. Phys.* **2016**, *16* (3), 1747–1760.
- (49) Kanakidou, M.; Seinfeld, J. H.; Pandis, S. N.; Barnes, I.; Dentener, F. J.; Facchini, M. C.; Van Dingenen, R.; Ervens, B.; Nenes, A.; Nielsen, C. J.; et al. Organic aerosol and global climate modelling: a review. *Atmos. Chem. Phys.* **2005**, *5* (4), 1053–1123.
- (50) Kourtchev, I.; Giorio, C.; Manninen, A.; Wilson, E.; Mahon, B.; Aalto, J.; Kajos, M.; Venables, D.; Ruuskanen, T.; Levula, J.; et al. Enhanced Volatile Organic Compounds emissions and organic aerosol mass increase the oligomer content of atmospheric aerosols. *Sci. Rep.* **2016**, *6*, 35038.
- (51) Kalberer, M.; Paulsen, D.; Sax, M.; Steinbacher, M.; Dommen, J.; Prévôt, A. S. H.; Fisseha, R.; Weingartner, E.; Frankevich, V.; Zenobi, R.; et al. Identification of polymers as major components of atmospheric organic aerosols. *Science* **2004**, *303* (5664), 1659–1662.
- (52) Kourtchev, I.; Doussin, J.-F.; Giorio, C.; Mahon, B.; Wilson, E. M.; Maurin, N.; Pangu, E.; Venables, D. S.; Wenger, J. C.; Kalberer, M. Molecular composition of fresh and aged secondary organic aerosol from a mixture of biogenic volatile compounds: a high-resolution mass spectrometry study. *Atmos. Chem. Phys.* **2015**, *15* (10), 5683–5695.
- (53) Giorio, C.; Monod, A.; Brégonzio-Rozier, L.; DeWitt, H. L.; Cazaunau, M.; Temime-Roussel, B.; Gratien, A.; Michoud, V.; Pangu, E.; Ravier, S.; et al. Cloud Processing of Secondary Organic Aerosol from Isoprene and Methacrolein Photooxidation. *J. Phys. Chem. A* **2017**, *121* (40), 7641–7654.